

# PV Output Smoothing using a Battery and Natural Gas Engine-Generator

Jay Johnson<sup>1</sup>, Abraham Ellis<sup>1</sup>, Atsushi Denda<sup>2</sup>, Kimio Morino<sup>2</sup>,  
Takao Shinji<sup>3</sup>, Takao Ogata<sup>3</sup>, and Masayuki Tadokoro<sup>3</sup>

<sup>1</sup>Sandia National Laboratories, Albuquerque, NM, 87185, USA

<sup>2</sup>Shimizu Corporation

<sup>3</sup>Tokyo Gas Co., Ltd.

**Abstract** — In some situations involving weak grids or high penetration scenarios, the variability of photovoltaic systems can affect the local electrical grid. In order to mitigate destabilizing effects of power fluctuations, an energy storage device or other controllable generation or load can be used. This paper describes the development of a controller for coordinated operation of a small gas engine-generator set (genset) and a battery for smoothing PV plant output. There are a number of benefits derived from using a traditional generation resource in combination with the battery: the variability of the photovoltaic system can be reduced to a specific level with a smaller battery and Power Conditioning System (PCS) and the lifetime of the battery can be extended. The controller was designed specifically for a PV/energy storage project (Prosperity) and a gas engine-generator (Mesa Del Sol) currently operating on the same feeder in Albuquerque, NM. A number of smoothing simulations of the Prosperity PV system were conducted using power data collected from the site. By adjusting the control parameters, tradeoffs between battery use and ramp rates could be tuned. A cost function was created to optimize the control in order to balance—in this example—the need to have low ramp rates with reducing battery size and operation.

**Index Terms** — photovoltaic systems, DER, PV smoothing, power control, optimization, microgrids

## I. INTRODUCTION

In rare situations involving weak grids or high penetration, local storage systems are introduced to mitigate adverse impacts due to variability of renewable generation on the electrical grid. These storage systems (e.g. batteries) smooth the renewable power output so that the local grid voltage (and frequency in the case of island grids) are not negatively impacted. As part of a DOE-sponsored energy storage demonstration, Public Service Company of New Mexico (PNM) has a 500 kW photovoltaic (PV) system co-located with a 500 kW, 330 kWh valve-regulated lead-acid (VRLA) smoothing battery [1] at the Prosperity site near the Albuquerque Airport. The battery is currently used to demonstrate smoothing of the PV power, using a control algorithm developed by Sandia [2]. The New Energy and Industrial Development Organization of Japan (NEDO), in partnership with PNM, the University of New Mexico, and

Sandia National Labs has developed a smart grid demonstration project at Mesa del Sol, to investigate, among other things, the benefits of using traditional generation in addition to storage to control PV power variability [3]. The Prosperity and Mesa del Sol projects are installed on the same 12.47 kV feeder. This report describes optimized operation of the gas engine-generator (genset) and the battery, with respect to factors such as the size of the battery, size of the battery inverter, and the lifetime of the battery. The Mesa del Sol and Prosperity projects are shown in Figure 1. The smoothing control was designed for the 500 kW power battery.

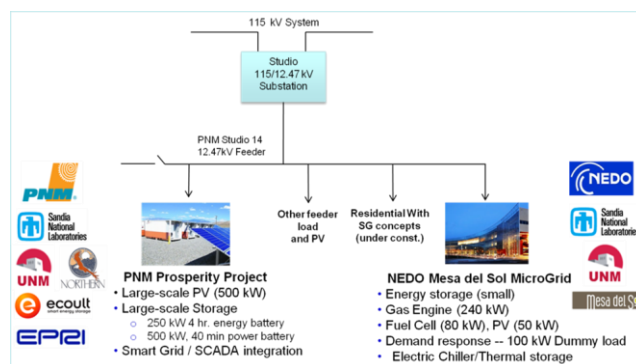


Fig. 1 Mesa del Sol distribution system.

The control algorithm currently employed by the battery system was an area of previous study [2]. This controller was modified to include the addition of the gas engine-generator (GE). In the extended control formulation, the gas genset receives the near real-time power signal from the Prosperity site and adjusts its power in conjunction with the battery to smooth the PV power output.

## II. SMOOTHING CONTROL ALGORITHM DESIGN

The use of battery to reduce the variability of PV and wind generation systems has been the subject of much research [3-6]. Recently, a few commercial PV and wind projects have been installed in Hawaii with co-located energy storage to

meet specific output variability limits at the point of common coupling (PCC) [7]. Other island jurisdictions are considering similar output variability limits that could drive need for energy storage or other mitigation alternative [8]. It should be noted that these requirements for ramp rate limits at the PCC are only applicable to specific circumstances where the variable generation project can cause local voltage or system frequency impacts. For larger interconnected grids, and even island grids, a more cost-effective use of energy storage systems would be to help maintain grid stability by supporting system voltage and frequency [9-10]. In the case of the Prosperity project, the PV system was co-located with a battery as a demonstration, to learn how a utility could manage distributed resources to contribute to various grid support objectives, including variability reduction or smoothing.

#### A. Combined Gas Engine-Generator and Battery Controller

The existing PNM battery-PV smoothing control [2] determines the desired power required from a controllable resource (battery) using a moving average sliding window or low-pass-filtered version of the PV power history. The idea is that the controllable resource would make up the difference between the PV power output and the smoothed power output profile (i.e., error signal). The difference between this implementation and the extended work described in this document is that both the battery and the gas engine-generator, as opposed to just the battery, respond to the error signal. The gas engine-generator is significantly slower than the PV and the battery, so it is only able to completely relieve the battery from operating during slow PV ramp rates. The faster ramp rates are still nearly fully tasked to the battery. After accounting for limitations such as engine-generator rating and battery state of charge (SOC) limits, the overall smoothing control formulation has several degrees of freedom. This means that control parameters can be optimized based on other factors like operational cost and battery lifetime. In the same manner, simulation-based optimization can be used to determine the required size of energy storage capacity and associated power conditioning system (PCS).

The 240 kW gas engine-generator requires a minimum output of 120 kW to operate with a reasonable efficiency and emissions levels. Accordingly, it is assumed that the gas engine-generator operates between 120 kW and 240 kW. When in operation, the gas engine-generator output has a return signal to adjust the output to a nominal value at the center of the operating range (e.g., 180 kW) so that it can respond in the positive and negative directions by reducing or increasing power output. For the purposes of smoothing, contribution of the gas engine-generator,  $P_{GE}$ , is defined as the power change from nominal, such that  $-60 \text{ kW} < P_{GE} < 60 \text{ kW}$ . In the actual implementation at Mesa del Sol, the genset power limits are enforced by a separate genset controller. Similarly, the controller should return the energy storage SOC to a nominal value near the center of the SOC range, at a rate that is slow compared to the energy storage ramping capability. For example, the SOC limits ( $SOC_{min}$  and  $SOC_{max}$ )

may be 20% and 80%, respectively, and the reference SOC ( $SOC_{ref}$ ) may be 50%. These SOC levels will vary on the application, battery technology, and smoothing controller design. In the actual implementation at Prosperity, the SOC limits are enforced by a separate battery energy system controller.

In summary, the real-time controller performs the following actions:

1. Determines the desired, smooth power of the system,  $P_{smooth}$ , using a moving average or low pass filter based on the time history of PV power,  $P_{PV}$ .
2. Issues power reference commands to the energy storage system and engine control to ensure the total power from the generators is nearly equal to the smoothed power profile:  $P_{smooth} \cong P_{pv} + P_{bat} + P_{GE}$ , where  $P_{bat}$  is the battery power and  $P_{GE}$  is defined as the GE power change from nominal, as described above.
3. Slowly, return the battery SOC and genset output to a nominal level, as described above.

The PV power error is defined by the difference in  $P_{smooth}$  and  $P_{PV}$  and will be approximately the power generated by the gas engine-generator and the battery. In an actual implementation,  $P_{error}$  cannot be expected to be zero at all times because of communication and processing delays, and limits imposed by the battery and genset controllers.

The controller is shown in Figure 2. As shown in the upper grey block of Figure 2, PV error signal (smoothing requirement) is calculated by the battery smoothing control, which is co-located with the PV and energy storage system. This error signal is transmitted to the gas engine-generator control. The output of the gas engine-generator control is subtracted from the error signal and transmitted to the battery smoothing control to compute the battery set point. This control architecture is suitable for the smoothing application because the gas engine-generator is much slower than the battery, so the battery can make up for the power that the GE is unable to produce. Further, battery life is more sensitive to power production than the GE, so this hierarchical structure helps extend the lifetime of the battery.

The gas engine-generator and battery controllers are similar. The error signal first is passed through a dead band which forces the error to reach a certain point before the controller responds. The dead band is set to zero for all simulations in this report. There is a gain that scales the error signal reaching the genset and battery. The scaling factor for the genset,  $GE_{gain}$ , varies in the simulations and the battery controller gain is set to unity (and therefore not shown in Figure 2). A scaling factor of unity for the energy storage smoothing control is reasonable for this particular project, given that the rating of the PV inverter the energy storage PCS are both 500 kW. The control signal is returned to  $P_{GE\_nom}$  and  $SOC_{ref}$  for the GE and battery using a proportional gain feedback control. The values of  $K_{GE}$  and  $K_{SOC}$  are small relative to the ramping capability of the genset and battery to ensure that smoothing control has priority, but over time return the GE to  $P_{GE\_nom}$  and the battery to  $SOC_{ref}$ . The resulting genset and battery power setpoints are sent to the gas engine-generator and battery plants. In the

simulations discussed in this paper, the energy storage is represented as a simple integrator, which ignores battery losses. Battery hardware-driven ramp limits are higher than requirements placed on the battery, so the limits are not represented in the simulations or in the model of the battery plant in Figure 2. For the purposes of the simulations discussed in this paper, the gas engine-generator is represented with a simple rate limit of 0.285 kW/second. This was based on performance tests. The genset operational limits are related to the engine performance and emissions considerations. Finally these control signals experience a communication delay before adjusting the power at the plant.

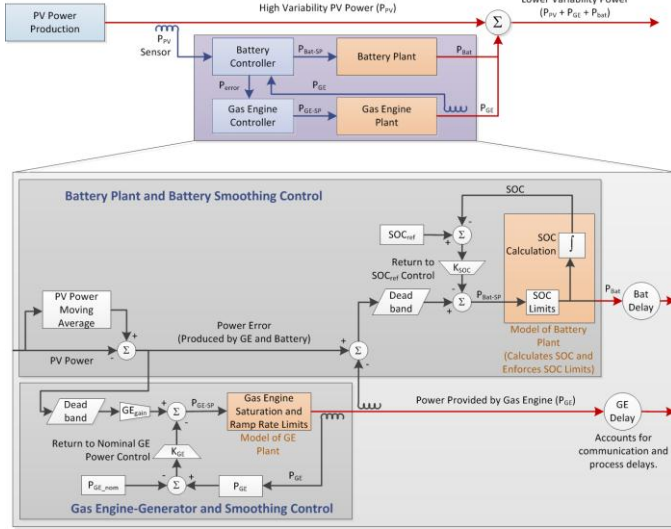


Fig. 2. Control scheme for the battery and gas engine-generator.

### III. GAS ENGINE-GENERATOR AND BATTERY SIMULATIONS

Prosperity PV output data from five different days was used to simulate smoothing using the gas engine-generator and battery. These simulations were used to identify appropriate ranges for control parameters to optimize the smoothing control. A simulation of one of the daily output profiles, shown in Figure 3, illustrates that the genset is not fast enough to keep up with the larger ramp rates and often saturates, but it does significantly reduce the SOC range of the battery, shown in the bottom plot. The PV output is depicted at the top image along with the smoothed profile. The middle image shows the battery operation with and without the help of the gas engine-generator.

The inability of the gas engine-generator to reduce the magnitude of fast PV output ramps can be clearly seen by examining the period after 2 PM in Figure 4, when there is a large ramp in the PV output due to a cloud shadow passing over the array. Even though the slow gas engine-generator cannot respond quick enough or with enough power to significantly counteract the  $P_{error}$  signal, the power output requirements of the battery are reduced by the gas engine-generator response. In this case, the SOC range of the battery

is reduced from 25.1% to 12.6% and the maximum PCS instantaneous power requirement is reduced from 292.6 to 260.4 kW. In a design situation, this means that the required size of the battery, the storage capacity of the battery, and the battery PCS can be reduced if a secondary generator such as a genset is available to assist with smoothing. Furthermore, in the case of smaller  $P_{error}$  ramps, as shown after 2:30 PM in Figure 5, the gas engine-generator can, at times, fully smooth the PV output and the battery does not have to be employed at all.

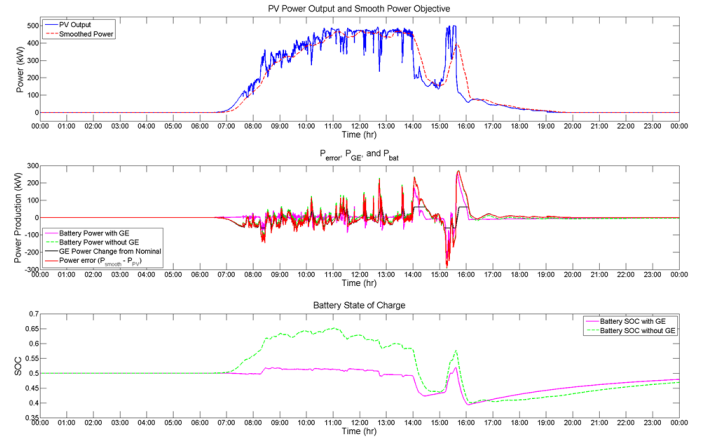


Fig. 3 The influence of the gas engine-generator on battery operation.

Figure 5 depicts a cumulative distribution function (CDF) of the 1-minute PV output ramps and the smoothing effect of the battery on PV output. Note that the reduction in variability needs to be defined in terms of a specific statistical term. A simple way is to compare the maximum ramps, however, this metric is subject to measurement noise and fault events (such as inverter trips). As a result, in this paper, a high percentile (i.e., the 99<sup>th</sup> percentile) of ramps is used as the smoothing metric. Additional discussion of ramp rates is provided in [11].

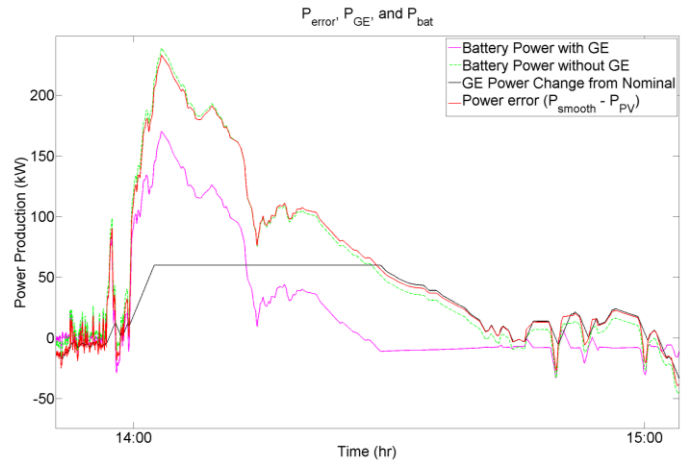


Fig. 4. Detail of Figure 3, showing power production from the battery and gas engine-generator.

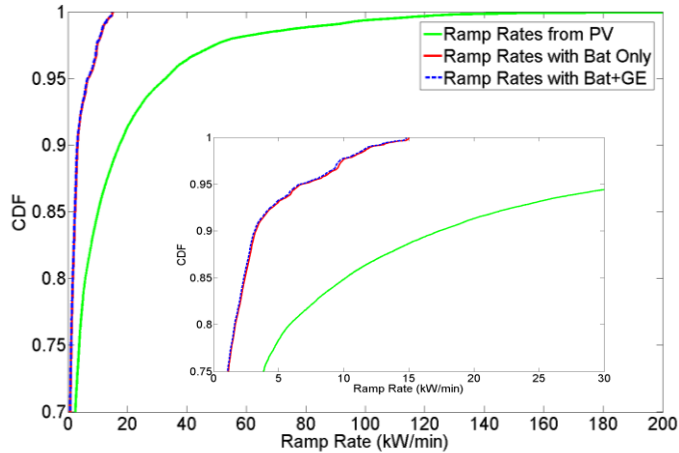


Figure 5. Cumulative distribution function of the 1-minute power ramp rates for the  $P_{PV}$ ,  $P_{PV}+P_{bat}$ , and  $P_{PV}+P_{bat}+P_{GE}$ .

### A. Influence of the Control Parameters

The simulations above indicate that traditional power generation such as a genset can be operated to supplement a battery to perform smoothing using a simple controller. To determine the optimal control for this application a number of parameters in the controller were adjusted to improve the performance. The parameters included in this study were:

1. **GE<sub>gain</sub>** – The amount of power error that the gas engine-generator attempts to eliminate.
2. **T<sub>w</sub>** – The window of time that the moving average uses to calculate  $P_{smooth}$ .
3. **K<sub>SOC</sub>** – The proportional controller used to return the battery to  $SOC_{ref}$ .
4. **K<sub>GE</sub>** – The proportional controller used to return the GE to the nominal GE power. This is selected to be a percentage of the maximum ramp rate of the GE,  $GE_{RRSat} = 0.285$  kW/s, so the smoothing control has priority over the GE return signal.
5. **GE Delay** – Amount of time that the GE takes to respond to a change in power setpoint,  $P_{GE-SP}$ .

The parameter values selected for these studies are shown in Table 1.

TABLE 1  
SUMMARY OF PARAMETERS FOR BATTERY + GE CONTROLLERS.

Parameter	Default Value	Range of Values
GE <sub>gain</sub>	1	0-1
T <sub>w</sub>	300 s	300-1800 s
K <sub>SOC</sub>	100	10-1000
K <sub>GE</sub>	0.2 · GE <sub>RRSat</sub>	0.05 · GE <sub>RRSat</sub> -0.5 · GE <sub>RRSat</sub>
GE Delay	0 s	0-5 s

### B. Figures of Merit

In order to optimize the control parameters, a number of figures of merit (FOMs) were defined to represent different performance metrics and costs. For instance, a system designer may be interested in balancing the cycle life

expectancy and size of the battery with the degree of PV smoothing and natural gas engine-generator usage. The FOMs used to represent various performance aspects of the design are as follows:

- **RR<sub>99</sub>**: The 99th percentile of the 1-minute ramp rate in kW/min for a given test period, e.g., one day with a high degree of PV output variability. (See [13] for details.) This is a good approximation of the degree of smoothing that the control system achieves.
- **BatSOCRange**: The range of battery capacity expressed as the difference between the minimum and the maximum SOC during the simulation. This is used to determine the required capacity of the battery.
- **MaxBatkW**: The maximum output power of the battery during the simulation. This defines the size of the PCS connected to the battery.
- **BatWork**: Total work done by the battery during the simulation in GJ as defined by:  $\int |P_{bat}| dt$ . This represents the amp-hour throughput of the battery and is one metric for predicting the lifetime of the battery [12].
- **AvgGEPower**: The average gas engine-generator power production in kW (referenced from nominal). This is a rough estimate—ignoring GE efficiencies—of additional fuel the GE uses compared to running at a nominal 180 kW level.
- **GEwear** = The amount of GE adjustment during the simulation,  $\int |P_{GE}| dt$ . Larger values indicate the GE power was adjusted more often or by larger amounts. This value is used as a surrogate for wear; although, genset operating time or total kWh could also be used [13].

The simple FOMs described above were developed to illustrate an optimization methodology. They can be further refined or different metrics could be selected that are more suitable for the specific situation.

### C. Control Optimization

Latin Hypercube Sampling (LHS) was employed to develop an intuitive understanding of the influence of the control parameters on the different figures of merit. The range of the design parameters is shown in Table 1. A total of 500 simulations using different control parameters were conducted for the 5 PV power profiles shown at the bottom of Figure 7.

Figure 6 shows the results of the LHS for Day 1. There is substantial information in Figure 6 relating the control parameters to the FOMs. A strong correlation between a parameter and a FOM indicate that parameter has a strong influence on that FOM. The vertical scatter in the plots is the influence of the other parameters on the FOM. Thus, when there is a large vertical scatter, the other parameters play a significant role in that FOM.

Some of the insights that can be gathered from Figure 6 include:

- When the GE is used, the battery does not work as hard (GE<sub>gain</sub> vs. BatSOCRange) or need to be as big (GE<sub>gain</sub> vs. MaxBatkW), and it improves the lifetime of the battery

because there are fewer amp-hours cycled through the battery ( $GE_{gain}$  vs.  $BatWork$ ).

- The GE is not fast enough to help with the highest ramp rates ( $GE_{gain}$  vs.  $RR_{99}$ ).
- The most critical factor in the ramp rates is the smoothing window size ( $T_w$  vs.  $RR_{99}$ ). For a larger smoothing window the ramp rates drastically decrease.
- Smoother power means more or larger GE power adjustments ( $T_w$  vs.  $GE_{wear}$ ) and more battery use ( $T_w$  vs.  $BatWork$ ).
- $K_{GE}$  and GE Delay have little influence on the FOMs based on the correlation values in the last two columns.
- The rate at which the battery returns to the SOC influences the battery FOMs and the ramp rates. For larger  $K_{SOC}$  values, the ramp rates increased slightly ( $K_{SOC}$  vs.  $RR_{99}$ ), the SOC range is reduced slightly ( $K_{SOC}$  vs.  $BatSOCRange$ ), the max battery power output increases ( $K_{SOC}$  vs.  $MaxBatkW$ ), but overall battery use is reduced ( $K_{SOC}$  vs.  $BatWork$ ).
- Smoother power equates to a need for more battery capacity ( $T_w$  vs.  $BatSOCRange$ ) and larger PCS size ( $T_w$  vs.  $MaxBatkW$ ).
- There are nonlinearities for some parameters ( $GE_{gain}$  vs.  $MaxBatkW$ ) possibly due to the PV profile for this particular day.
- The GE works harder when it is responding more aggressively to the  $P_{error}$  signal ( $GE_{gain}$  vs.  $GE_{wear}$ ).
- Less genset power is required when the GE is used for smoothing compared to running at nominal power ( $GE_{gain}$  vs.  $AvgGEPower$ ), possibly because  $\int P_{error} dt$  is negative so there is more need to reduce power than increase power for this day and/or the GE follows the error signal better in morning when it is less cloudy (lower ramp rates) and  $P_{error} < 0$ .
- $K_{SOC}$ ,  $K_{GE}$  and GE Delay have very little impact on the FOMs defined for this example.

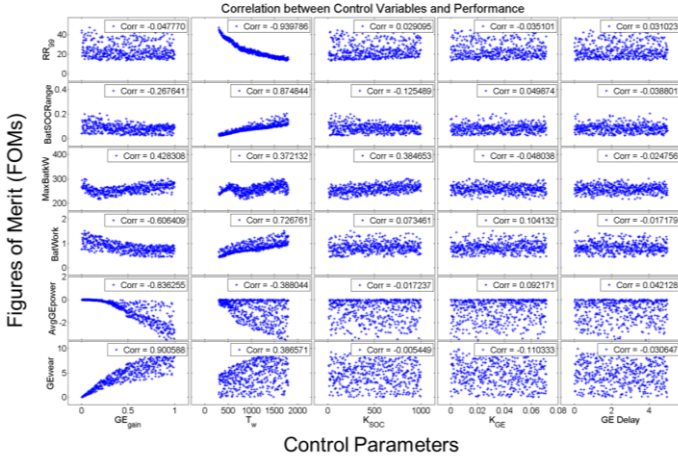


Fig. 6. Latin Hypercube Sampling results for Day 1.

Figure 7 compares the results of the LHS for all five days. The figure shows there are similar trends for the other four days and some of the FOMs are heavily influenced by the PV power output profile. When there is stratification in the LHS

matrix it indicates that those FOMs are driven by the PV power profile and not solely by the controller. For instance, the largest ramp rates can be mitigated with larger  $T_w$  values, but days with more clouds tend to produce larger ramp rates for smaller  $T_w$  values. Similarly, the maximum instantaneous battery output and total work is closely correlated to the days with larger ramp rates. These results also confirm that  $K_{SOC}$ ,  $K_{GE}$  and GE Delay have very little effect on the FOMs.

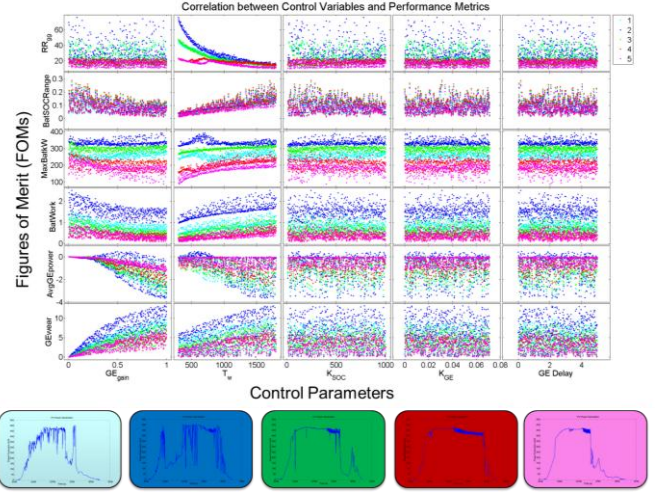


Fig. 7. Latin Hypercube results for all 5 days.

To determine the optimal control for the Mesa del Sol system, a cost function based on weighted FOMs factors with additional constraints on FOMs was created. The function and constraints will vary with hardware, climate, and objectives of the owner. For instance, it may be necessary to reduce the ramp rates to a specific level, but this will cycle the battery more and reduce the expected battery cycle life. If larger PV output ramps are acceptable, the battery life could be extended.

As an example, consider a situation where energy storage system is being considered to limit PV ramps to 50 kW/min and there is interest in minimizing the battery size while still having a reasonable battery cycle life expectancy. Let's assume that a genset with the characteristics discussed in Section 1 is available, and the control scheme described in Figure 2 is employed. The control fitness function for simulation,  $i$ , is,

$$F_i = K_{RR,i} \cdot [f(BatSOCRange_i) + f(BatWork_i)] \quad (1)$$

where

$$K_{RR,i} = \begin{cases} 1 & \text{if } RR_{99,i} < 50 \text{ kW/min} \\ 0 & \text{if } RR_{99,i} > 50 \text{ kW/min} \end{cases} \quad (2)$$

$$f(BatSOCRange_i) = w_1 \left( \frac{\max(BatSOCRange) - BatSOCRange_i}{\max(BatSOCRange)} \right) \quad (3)$$

$$f(\text{BatWork}_i) = w_2 \left( \frac{\max(\text{BatWork}) - \text{BatWork}_i}{\max(\text{BatWork})} \right) \quad (4)$$

where  $\max(\text{BatSOCRange})$  and  $\max(\text{BatWork})$  values are the largest outputs from the LHS results and used to normalize  $f(\text{BatSOCRange}_i)$  and  $f(\text{BatWork}_i)$ . The weightings  $w_1$  and  $w_2$  were selected based on the relative importance of minimizing the battery size and increasing battery life. Here,  $w_1$  was selected to be 10 and  $w_2$  was 3. The fitness of a controller was designed to be 0 if the controller was unable to keep system power ramps below the design requirement. If the controller kept ramp rates below 50 kW/min, then the largest  $F_i$  value balanced the battery size and lifetime.

It should also be noted that this optimization process can also be performed prior to the construction of the PV system. The PV power output can be predicted using irradiance data collected at the site [14] and the battery and gas engine-generator outputs can be simulated in MATLAB/Simulink.

To make the optimization process simpler, the number of input parameters was reduced to  $GE_{\text{gain}}$ ,  $T_w$ , and  $K_{\text{SOC}}$ , because  $K_{\text{GE}}$  and GE Delay did not significantly influence  $RR_{99}$ ,  $\text{BatSOCRange}$ , or  $\text{BatWork}$ . A sequential quadratic programming (SQP) optimizer was wrapped around the Simulink simulation for the most variable day (day 2), and the optimal controller was determined to be  $T_w = 444.83$ ,  $GE_{\text{gain}} = 0.531$ , and  $K_{\text{SOC}} = 10.0$ . This indicates that the lowest  $T_w$  values were not suitable for the controller because the ramp rates are too large, but being close to the 50 kW/min limit is desirable because it minimizes the battery size and battery use. If the 50 kW/min limit was a critical boundary (e.g., there would be a contract violation if it was exceeded), then it would likely be better to find a more robust controller with a larger  $T_w$ , so that in the event of high solar variability, the maximum ramps requirement would not be crossed.

#### IV. CONCLUSIONS

Simulations of PV power smoothing control strategies were performed in MATLAB/Simulink to demonstrate the influence of different control parameters on figures of merit. The controller utilizes both a traditional natural gas genset and a battery to perform the smoothing. The smoothed power target is calculated using a sliding window on the time history of the PV plant output. Using the gas engine-generator in addition to just a battery for PV power smoothing provides a number of benefits including longer battery life, smaller power conditioning system, and smaller battery capacity.

The simulations show that certain targets (e.g. specific ramp rates) can be reached and the entire system can be optimized by adjusting the control parameters. Some control parameters were found to influence the figures of merit more than others. Most critical control parameters on the figures of merit were the amount of GE use, battery SOC return signal, and, most importantly, sliding window size. The control parameters could be tuned to minimize battery and GE use or decrease the system ramp rates. These trade-offs were considered to find

an optimal control for a theoretical set of constraints and design objectives.

#### REFERENCES

- [1] O. Lavrova, et al., "Modeling of PV plus Storage for Public Service Company of New Mexico's Prosperity Energy Storage Project," 2011 EESAT, San Diego, CA, Oct. 16-19, 2011.
- [2] A. Ellis and D. Schoenwald, PV Output Smoothing with Energy Storage, Sandia Technical Report, SAND2012-1772, March 2012.
- [3] S. Abdollahy, A. Mammoli, F. Cheng, A. Ellis, and J. Johnson, Distributed Compensation of a Large Intermittent Energy Resource in a Distribution Feeder, IEEE PES Innovative Smart Grid Technologies (ISGT), 24-27 Feb., 2013.
- [4] T. Hund, S. Gonzalez, and K. Barrett, "Grid-Tied PV System Energy Smoothing," 35th IEEE PVSC, Honolulu, HI, pp. 2762-2766, June 20-25, 2010.
- [5] H. Fakhm, D. Lu, and B. Francois, "Power Control Design of a Battery Charger in a Hybrid Active PV Generator for Load-Following Applications," IEEE Transactions on Industrial Electronics, vol. 58, no. 1, pp. 85-94, Jan. 2011.
- [6] M. Khalid and A.V. Savkin, Renewable Energy, vol. 35, no. 7, pp. 1520-1526, July 2010.
- [7] KEMA, Inc., Lanai PV Interconnect Requirements Study: System Impact Study, June 5, 2008, Interconnection Customer: SunPower, KEMA, Inc., Raleigh, NC, USA, 26707.
- [8] Puerto Rico Electric Power Authority, Minimum Technical Requirements for Interconnection of Photovoltaic Facilities, 2012.
- [9] M. Coddington and A. Ellis, Updating Interconnection Screens for PV Integration Con Streamline Deployment, Solar Industry, vol. 5, no. 8, pp. 70-74, Sept. 2012.
- [10] P. Denholm, E. Ela, B. Kirby, and M. Milligan, The Role of Energy Storage with Renewable Electricity Generation, NREL Technical Report, NREL/TP-6A2-47187, January 2010.
- [11] J. Johnson, B. Schenkman, A. Ellis, J. Quiroz, and C. Lenox, "Initial Operating Experience of the 1.2-MW La Ola Photovoltaic System," 38th IEEE PVSC, Austin, TX, 2012.
- [12] H. Bindner, T. Cronin, P. Lundsager, J.F. Manwell, U. Abdulwahid, and I. Baring-Gould, Lifetime modelling of lead acid batteries. Risø-R Report, Risø-R-1515(EN), 2005.
- [13] M. Muselli, G. Notton, A. Louche, Design of hybrid-photovoltaic power generator, with optimization of energy management, Solar Energy, vol. 65, no. 3, pp 143-157, 1 Feb. 1999.
- [14] C.W. Hansen, J.S. Stein, and A. Ellis, Simulation of 1-Minute Power Output from Utility-Scale Photovoltaic Generation Systems, SAND2011-5529, Sandia National Laboratories, Albuquerque, NM, 2011.

#### ACKNOWLEDGEMENT

Sandia National Laboratories is a multi-program laboratory managed and operated by Sandia Corporation, a wholly owned subsidiary of Lockheed Martin Corporation, for the U.S. Department of Energy's National Nuclear Security Administration under contract DE-AC04-94AL85000. We acknowledge the contribution of Public Service Company of New Mexico and Japan's New Energy and Industrial Development Organization (NEDO) for providing access to critical data.